

**Spin relaxation of free excitons in narrow GaN/Al<sub>x</sub>Ga<sub>1-x</sub>N quantum wells**

J. Besbas, A. Gadalla,\* M. Gallart,† O. Crégut, B. Hönerlage, and P. Gilliot  
 IPCMS–DON Unité Mixte, UMR 7504, CNRS–ULP, 23 rue du Læss, BP 43, 67034 Strasbourg Cedex 2, France

E. Feltin, J.-F. Carlin, R. Butté, and N. Grandjean

ICMP, Ecole Polytechnique Fédérale de Lausanne (EPFL), CH-1015 Lausanne, Switzerland

(Received 17 May 2010; revised manuscript received 7 October 2010; published 3 November 2010)

By performing pump-probe experiments, we study the relaxation dynamics of spin-polarized excitons in a wurtzite GaN/AlGa<sub>N</sub> quantum well (QW) grown by metal organic vapor phase epitaxy. The circular degree of polarization of the differential reflectivity signal reaches 55–60 % for the heavy-hole exciton when it is resonantly excited before decaying in a few picoseconds. This is an indication that, even if excitons are confined in the growth direction, their propagation in the well plane makes them very sensitive to scattering processes which are responsible for exciton dephasing and, therefore, for efficient spin relaxation. Above 80 K the thermal escape of excitons toward the AlGa<sub>N</sub> barrier increases the spin-relaxation rate. However, when compared to bulk GaN epilayers, where no spin polarization could be detected above 50 K, the optical orientation is preserved in those QWs up to about 100 K.

DOI: [10.1103/PhysRevB.82.195302](https://doi.org/10.1103/PhysRevB.82.195302)

PACS number(s): 78.47.jg, 78.67.De, 72.25.Fe, 72.25.Rb

**I. INTRODUCTION**

GaN and related materials have emerged as one of the most successful systems for optoelectronic applications in the UV-visible spectral range. Their weak spin-orbit coupling and large exciton binding energy ( $\sim 26$  meV in bulk GaN) also make them promising candidates for spintronic applications that require to control and manipulate the exciton spin at room temperature. This is partly due to the reduced spin-orbit splitting  $\Delta_{SO}$  at the  $\Gamma$  point of the Brillouin zone which is as small as  $\sim 17$  meV.<sup>1,2</sup>

Spin physics has been mostly investigated in bulk III-nitride materials. Previous work has shown that the spin lifetime of free excitons in undoped GaN epilayers lies in the picosecond range<sup>3–6</sup> and our group has demonstrated that a high dislocation density could enhance the exciton spin-relaxation rate in GaN through the Elliott-Yafet mechanism.<sup>7–9</sup>

On the other hand, spin-dynamics measurements performed on *n*-doped GaN epilayers led to spin lifetime and spin-coherence time significantly longer than in undoped samples.<sup>10,11</sup> In these works, the spin polarization of the electron gas lasts after the photogenerated excitons have recombined.

Concerning nanostructures, ensembles of self-organized zinc-blende GaN/AlN quantum dots were studied by time-resolved photoluminescence<sup>12</sup> and the optical orientation of the exciton spin was measured. Under quasiresonant excitation conditions by polarized light, the linear polarization of the luminescence was preserved over the experimental nanosecond range even at room temperature. However, the linear degree of polarization was very low (10–20 %).

A recent work by Brown *et al.*<sup>13</sup> was devoted to spin dynamics in InGa<sub>N</sub>/GaN quantum wells (QWs) and InGa<sub>N</sub> epilayers. The spin lifetime was shown to lie in the picosecond time scale. However, InGa<sub>N</sub>-based semiconductor structures present very specific physical properties related to carrier localization in the ternary alloy, which makes the comparison with other systems difficult (see for instance Ref.

14 and references therein). To our knowledge, to date there are no experimental data concerning the spin dynamics in high-quality GaN/AlGa<sub>N</sub> QWs.

**II. SAMPLE CHARACTERISTICS AND EXPERIMENTAL PUMP-PROBE SETUP**

The sample we studied is a high quality, low Al content, GaN/AlGa<sub>N</sub> QW grown by metal organic vapor phase epitaxy (MOVPE) on *c*-plane sapphire substrate. The template is composed of a standard 3  $\mu$ m GaN buffer layer and a 200-nm-thick Al<sub>x</sub>Ga<sub>1-x</sub>N layer. A single GaN QW with a nominal thickness of 2.6 nm was then deposited and capped with a 50-nm-thick Al<sub>x</sub>Ga<sub>1-x</sub>N layer with  $x=5\%$ . The thickness gradient of the well region across the sample leads to accessible thicknesses which vary from 1.5 to 2.9 nm. As a result, the energy of the exciton recombination can be efficiently tuned by moving the spot of the optical beams over the sample. The dislocation density, determined by means of atomic force microscopy, is  $\sim 7 \times 10^8$  cm<sup>-2</sup>. Details on the growth and on the interface structure can be found in Ref. 15. The sample was characterized by low-temperature linear spectroscopy. Photoluminescence (PL) was excited by the second harmonic of an optical parametric amplifier (OPA) that was tuned at 640 nm (see below for more details on the pulsed laser source). A tungsten lamp was used for reflectivity measurements. In photoluminescence excitation spectroscopy (PLE) measurements, the emission of a xenon lamp was spectrally filtered by a monochromator to obtain a tunable photon energy with a 4 meV bandwidth (more detail on the PLE experiment can be found in Ref. 16). In all linear spectroscopy experiments, the light collected was dispersed in a spectrometer and detected by a cooled charge-coupled device camera. We used an Oxford MG11 cryostat in which the sample was surrounded by cold gaseous helium. Low-temperature ( $T=7$  K) linear optical spectra are shown in Fig. 1. In the reflectivity spectrum, two spectral structures, characteristic of QW excitons, are centered about 3.540 eV,

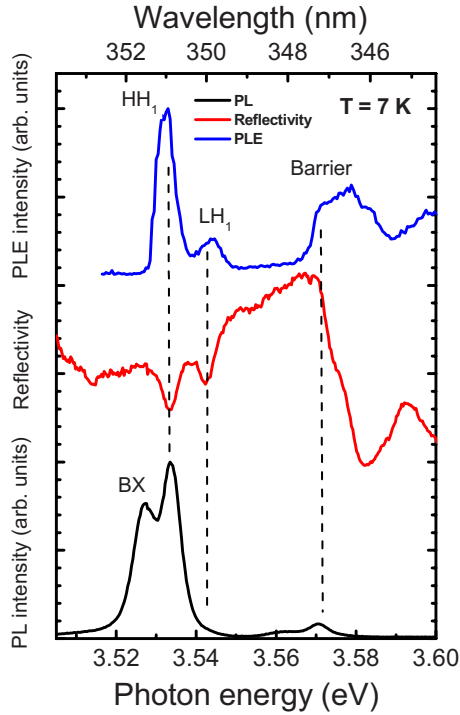


FIG. 1. (Color online) Photoluminescence, reflectivity and PLE spectra measured at  $T=7$  K.

above the GaN band gap. This is an experimental evidence that in this narrow QW the quasi-two-dimensional quantum confinement is stronger than the quantum-confined Stark effect (QCSE). The excitons are built from the first heavy- and light-hole confined states ( $HH_1$  and  $LH_1$ ), respectively, but they share the same first confined electronic state  $E_1$ . Their energies are split by 10 meV. Note that, in wurtzite bulk material,  $\Delta_{CR}$  and  $\Delta_{SO}$  lift the valence-band degeneracy at the  $\Gamma$  point. From the three valence subbands, possessing the  $\Gamma_9$ ,  $\Gamma_7$ , and  $\Gamma_7$  symmetry, and the  $\Gamma_7$  conduction band, one can build three exciton series labeled A, B, and C. The A exciton is the equivalent of the heavy-hole exciton in zinc-blende structures, while the B and C excitons are mixed, even at  $\mathbf{k}=0$ . In QWs, several confined states can be built from a valence band. With this in mind, we have chosen to identify the A and B excitons with HH and LH excitons, respectively, by analogy with zinc-blende QWs. The AlGaIn barrier also presents a signature at 3.59 eV in the reflectivity spectrum. All these features come along with a PL counterpart. The barrier PL exhibits a low-energy tail that could be due either to exciton localization by alloy disorder or to biexciton recombination.<sup>17</sup> To clarify this point, we have studied how the intensity of the low energy component of the barrier PL behaves when the power density varies. At low-excitation power, the PL intensity increases linearly with the excitation power indicating that exciton recombination tends to dominate. Also, we attribute to exciton localization the fact that this luminescence band is shifted to lower energies compared to the AlGaIn band gap. However, a quadratic dependence of the PL intensity appears with increasing power density showing that biexciton recombination dominates the low-energy side of the barrier PL for high excitation powers. The PL line shape also becomes more structured enabling us to extract a

biexciton binding energy equal to 10 meV, in good agreement with values determined in Ref. 17. In the case of the QW, one intense PL line corresponding to the  $HH_1$ -exciton recombination is observed. The line that is located 7 meV below the  $HH_1$  exciton displays a super linear dependence with the excitation power. It was interpreted in a previous work as the recombination of biexcitons.<sup>18</sup> A small PL signal is also issued from the  $LH_1$  exciton. The PLE spectrum obtained for a detection energy set to the emission energy of the  $HH_1$  exciton exhibits the signatures of the  $HH_1$  and  $LH_1$  excitons as well as that of the barrier and reveals that no additional confined excitonic states are present in the QW. No Stokes shift is observed for the above-mentioned transitions when comparing PL and PLE spectra. Note that previous work by Stokker-Cheragi *et al.*<sup>18</sup> on the same sample revealed a 3 meV Stokes shift for the  $HH_1$  exciton deduced from a comparison between PL and PLE spectra but the spectral resolution of our PLE setup ( $\sim 4$  meV) does not enable us to measure it. This slight Stokes shift ( $< QW$  PL linewidth  $\sim 5$  meV) is caused by the localization of the exciton center of mass in the QW plane. However, in the following pump-probe experiments, the density of excitons that are photocreated by the pump pulse is large enough to saturate the density of localized states and to populate free excitonic states.<sup>19</sup> Consequently, the changes in the probe reflectivity that we measure in nonlinear experiments, are essentially due to variations in the free exciton oscillator strength.

The pump-probe experimental procedure is identical to the one employed in our previous investigations.<sup>7,20,21</sup> The laser source includes a homemade titanium: sapphire oscillator. It generates 80 fs pulses at 82 MHz which pass a regenerative amplifier, working at 200 kHz, before being sent into two OPAs, tuned close to 700 nm (1.770 eV), that generate pump and probe pulses, respectively. Both of them are frequency doubled with two  $\beta$ -barium borate (BBO) crystals to reach the GaN exciton spectral region. The pulse duration is estimated to be  $\sim 200$  fs. The spectrum of the probe pulses is broad (17 meV of full width at half maximum) and spans the entire spectral region that is related to active excitonic transitions in the QW. To measure the spin dynamics, the pump pulses are circularly polarized and thus excite the  $HH_1$ -excitonic transition with total angular momentum  $|+1\rangle_{HH_1}$ . The energy per pulse is  $\sim 3$  nJ, and, after focusing onto the sample, it corresponds to  $\sim 1.8 \times 10^{14}$  photons  $\text{cm}^{-2}$  at an energy of 3.535 eV. The two circular components of the reflected probe pulses are recorded simultaneously as a function of the pump-probe delay time. For each time delay, the two reflected probe spectra are recorded in the presence and then in the absence of the pump pulse excitation and two differential reflectivity (DR/R) spectra are calculated, one for each circular probe polarization ( $\sigma^+$  and  $\sigma^-$ ). In all measurements, the sample was held in a cold-finger cryostat at low temperatures.

### III. EXCITON LIFETIME

Before studying the spin dynamics of QW excitons, we first determined their lifetime by using the same pump-probe

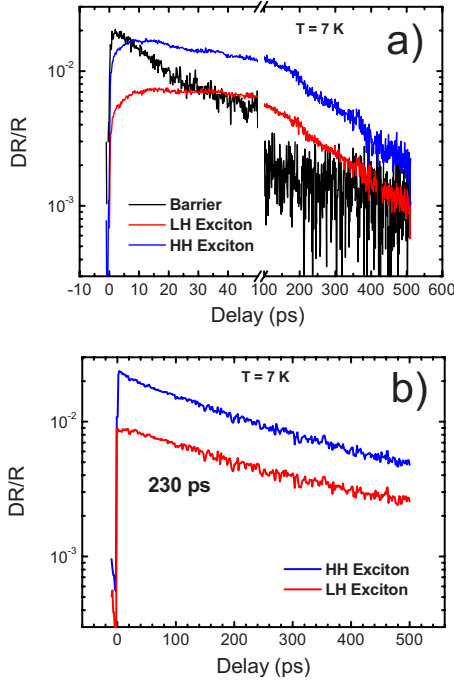


FIG. 2. (Color online) DR/R time evolutions of HH<sub>1</sub>, LH<sub>1</sub>, and barrier excitons (a) for excitation above the barrier and (b) for resonant excitation in the QW.

experimental setup with linearly polarized beams. The time evolutions of the DR/R signals associated with HH<sub>1</sub>, LH<sub>1</sub>, and barrier excitons are plotted in Fig. 2. Figure 2(a) corresponds to an excitation energy larger than the barrier band gap while Fig. 2(b) corresponds to resonant excitation of the QW excitons. When excitons are created in the barrier, the DR/R signals of HH<sub>1</sub> and LH<sub>1</sub> excitons exhibit a risetime that is characteristic of the population relaxation from the barrier toward the QW. It takes ~30 ps before the pump-probe signal begins to decay. When resonantly exciting QW excitons, the risetime is nothing more than the duration of the pump pulse. Whatever the excitation conditions (resonant or nonresonant), the signal decay for both HH<sub>1</sub> and LH<sub>1</sub> excitons is monoexponential with a time constant equal to 230 ps in good agreement with time-resolved photoluminescence experiments.<sup>22</sup> This short lifetime is an indication that the exciton oscillator strength remains substantial for a nitride based QW. It means that, in spite of the QCSE, the well width is sufficiently narrow to ensure a strong overlap of the electron and hole envelope wave functions along the growth axis of the QW.

IV. OPTICAL ORIENTATION

Figure 3(a) displays the DR/R spectra at a positive pump-probe time delay of 0.5 ps for the two different probe helicities, when the sample is excited with circularly polarized pulses. We assume that phase space filling is the nonlinear process responsible for the signal, the amplitude of which depends on the probe polarization, as expected from the QW optical selection rules. This indicates that a spin-polarized population of excitons is indeed photogenerated. For longer

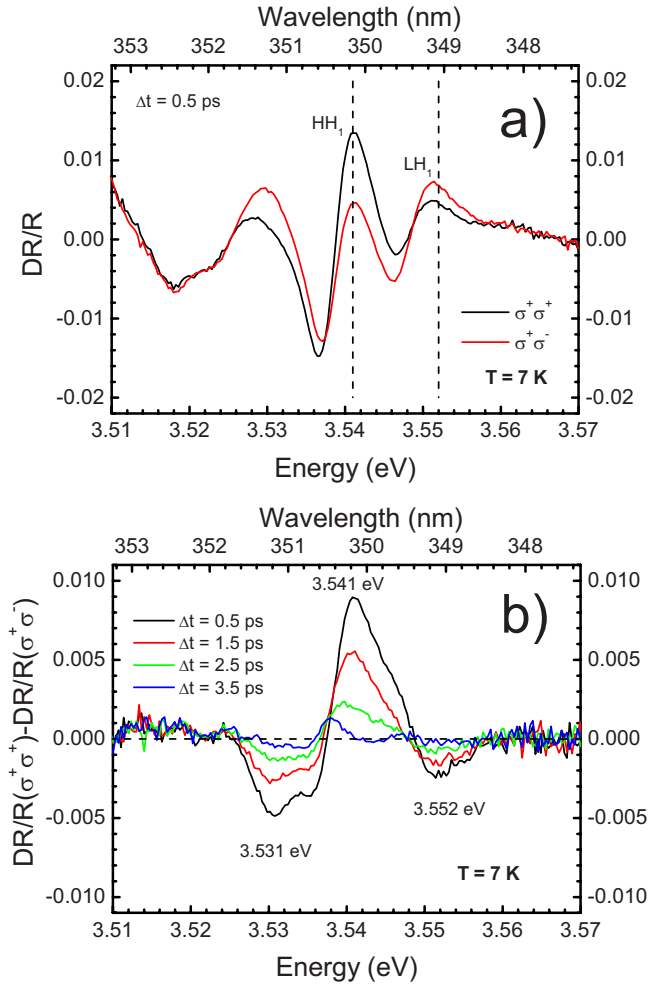


FIG. 3. (Color online) (a) DR/R spectra measured at a positive time delay of 0.5 ps for the two different probe helicities. (b) Difference between the DR/R spectra related to the two probe helicities  $(DR/R)(\sigma^+\sigma^+) - (DR/R)(\sigma^+\sigma^-)$  at different pump-probe delays.

time delays, the optical orientation disappears and the two spectra become identical.

We have also plotted in Fig. 3(b) the difference  $(DR/R)(\sigma^+\sigma^+) - (DR/R)(\sigma^+\sigma^-)$  for different pump-probe delays. Using this representation, even slight differences between the two spectra become noticeable. In the present case, it makes possible to observe three different transitions: the signals at 3.541 and 3.552 eV originate from the saturation of the HH<sub>1</sub> and LH<sub>1</sub> excitons, respectively. One also notices a signal, ~10 meV below the HH<sub>1</sub> resonance, which is stronger in counter polarized configuration of the pulses. This is characteristic of an induced exciton-biexciton transition as seen in previous work.<sup>7,8,23</sup> As expected, the amplitude of the nonlinear signal related to the HH<sub>1</sub> exciton is larger when the probe is  $\sigma^+$  polarized, (i.e., when it is copolarized with the pump) while it is the opposite for the LH<sub>1</sub> exciton (see below for a brief description of the spin structure of excitons). At short delay times (0.5 ps), the HH<sub>1</sub> signal is broad, showing that the photogenerated exciton distribution that contributes to the polarization of the DR/R signal extends over a wide spectral region (~10 meV). For longer time delays, a narrow distribution persists at lower energy on a time scale

>10 ps. This suggests that the most important part of the DR/R signal originates from free excitons that relax their pseudospin within a few picoseconds while a small portion of excitons keeps its optical orientation on a longer time scale. It could also be due to the polarization of electrons: indeed, a recent work by Buß *et al.*<sup>11</sup> suggests that, in GaN, the spin polarization of the electron gas due to the unintentional  $n$ -type doping can persist for hundreds of picoseconds, even for very low doping levels. Unfortunately, we do not have any additional data to explain this persistence of the spin orientation. Therefore, this minor feature is not investigated in this paper. Priority is thus given to the study of the fast component of the spin relaxation.

We briefly recall the spin structure of HH and LH excitons. Their electrons have a  $S_z = \pm 1/2$  spin and they involve heavy holes with pseudospin  $J_z = \pm 3/2$  and light holes with  $J_z = \pm 1/2$ , respectively. The resulting exciton pseudospin states  $|\pm 1\rangle_{\text{HH}_1}$ ,  $|\pm 1\rangle_{\text{LH}_1}$  are optically active while the  $|\pm 2\rangle_{\text{HH}_1}$  states and the twofold degenerate  $|0\rangle_{\text{LH}_1}$  state are dark states when exciting the sample with the electric field polarization perpendicular to  $\mathbf{c}$ . Because HH<sub>1</sub> and LH<sub>1</sub> excitons share the same conduction band, a population of  $|+1\rangle_{\text{HH}_1}$  excitons also modifies the oscillator strength of the  $|-1\rangle_{\text{LH}_1}$  excitons. Qualitatively, a simple model<sup>20</sup> based on fermionic phase space filling by electrons and holes gives the amplitudes of the DR/R signals, as a function of the electron and hole occupation numbers  $f_e$  and  $f_h$

$$\left(\frac{\text{DR}}{\text{R}}\right)_{\text{HH}_1}(\sigma^\pm) \propto F_{\text{OSC}}^{\text{HH}_1} \left[ f_e \left( \mp \frac{1}{2} \right) + f_h \left( \pm \frac{3}{2} \right) \right],$$

$$\left(\frac{\text{DR}}{\text{R}}\right)_{\text{LH}_1}(\sigma^\pm) \propto F_{\text{OSC}}^{\text{LH}_1} \left[ f_e \left( \mp \frac{1}{2} \right) + f_h \left( \mp \frac{1}{2} \right) \right],$$

where  $F_{\text{OSC}}$  denotes the excitonic oscillator strength. Next, we introduce  $n_{\text{HH}_1}(\pm 1)$  and  $n_{\text{LH}_1}(\pm 1)$ , the number of optically active heavy- and light-hole excitons, respectively. The parameter  $\pm 1$  refers to the total angular momentum of the exciton.  $n_{\text{HH}_1}(\pm 2)$  and  $n_{\text{LH}_1}(0)$  correspond to the number of dark excitons. The signals thus become

$$\left(\frac{\text{DR}}{\text{R}}\right)_{\text{HH}_1}(\sigma^\mp) \propto F_{\text{OSC}}^{\text{HH}_1} [2n_{\text{HH}_1}(\mp 1) + n_{\text{LH}_1}(\pm 1) + n_{\text{HH}_1}(+2) + n_{\text{HH}_1}(-2) + n_{\text{LH}_1}(\mp 0)],$$

$$\left(\frac{\text{DR}}{\text{R}}\right)_{\text{LH}_1}(\sigma^\mp) \propto F_{\text{OSC}}^{\text{LH}_1} [n_{\text{HH}_1}(\pm 1) + n_{\text{HH}_1}(\mp 2) + 2n_{\text{LH}_1}(\mp 1) + n_{\text{LH}_1}(+0) + n_{\text{LH}_1}(-0)].$$

LH<sub>1</sub> and HH<sub>1</sub> excitons are populated by the pump pulse and, at zero delay time, before any spin flip occurs, no dark excitons are present. Therefore, the signals read

$$\left(\frac{\text{DR}}{\text{R}}\right)_{\text{HH}_1}(\sigma^\mp) \propto F_{\text{OSC}}^{\text{HH}_1} \times [2n_{\text{HH}_1}(\mp 1) + n_{\text{LH}_1}(\pm 1)],$$

$$\left(\frac{\text{DR}}{\text{R}}\right)_{\text{LH}_1}(\sigma^\mp) \propto F_{\text{OSC}}^{\text{LH}_1} \times [2n_{\text{LH}_1}(\mp 1) + n_{\text{HH}_1}(\pm 1)].$$

Using these expressions, it is easy to see that, even in the absence of LH<sub>1</sub> excitons, a signal is expected at the LH<sub>1</sub>-exciton energy for a  $\sigma^-$ -polarized probe. The amplitude is equal to the amplitude of the HH<sub>1</sub> signal multiplied by the factor  $F_{\text{OSC}}^{\text{LH}_1}/2F_{\text{OSC}}^{\text{HH}_1}$ . For a  $\sigma^+$  pump excitation, at zero delay time, the population of  $|-1\rangle$  excitons is zero:  $n_{\text{LH}_1}(-1) = n_{\text{HH}_1}(-1) = 0$ . It is straightforward to show that, for a given type of exciton (HH<sub>1</sub> or LH<sub>1</sub>), the ratio  $(\text{DR}/\text{R})(\sigma^+)/(\text{DR}/\text{R})(\sigma^-)$  simply depends on  $n_{\text{HH}_1}(+1)$  and  $n_{\text{LH}_1}(+1)$  as follows:

$$\left(\frac{\text{DR}}{\text{R}}\right)_{\text{HH}_1}^{\sigma^+} / \left(\frac{\text{DR}}{\text{R}}\right)_{\text{HH}_1}^{\sigma^-} \propto 2 \frac{n_{\text{HH}_1}(+1)}{n_{\text{LH}_1}(+1)},$$

$$\left(\frac{\text{DR}}{\text{R}}\right)_{\text{LH}_1}^{\sigma^+} / \left(\frac{\text{DR}}{\text{R}}\right)_{\text{LH}_1}^{\sigma^-} \propto 2 \frac{n_{\text{LH}_1}(+1)}{n_{\text{HH}_1}(+1)}.$$

From the experimental data, we deduce that  $n_{\text{HH}_1}(+1) \sim 3.5 \times n_{\text{LH}_1}(+1)$ . Thus we conclude that the ratio  $F_{\text{OSC}}^{\text{LH}_1}/F_{\text{OSC}}^{\text{HH}_1}$  is close to 1, which would correspond to nearly equal radiative lifetimes for HH<sub>1</sub> and LH<sub>1</sub> excitons.

## V. SPIN RELAXATION

The spectrally integrated DR/R decays for the three QW transitions (HH<sub>1</sub>, LH<sub>1</sub>, and biexciton ones) are displayed in Fig. 4. The circular degree of polarization (CDP) defined as

$$\frac{\frac{\text{DR}}{\text{R}}(\sigma^+) - \frac{\text{DR}}{\text{R}}(\sigma^-)}{\frac{\text{DR}}{\text{R}}(\sigma^+) + \frac{\text{DR}}{\text{R}}(\sigma^-)}$$

is also plotted. It directly reflects the spin polarization of the exciton population.

First, we investigate the induced transition at the biexcitonic resonance. It reaches a maximum in  $\sigma^+\sigma^-$  configuration after a risetime of 0.8 ps. For a  $\sigma^+\sigma^+$  polarization sequence, it progressively increases while the  $\sigma^+\sigma^-$  DR/R signal decreases. The two signals are equal after 4 ps. According to the optical selection rules, there are two possible scenarios to create a biexciton starting from a  $|+1\rangle_{\text{HH}_1}$  exciton. It can follow the absorption of a  $\sigma^-$  probe photon or come about by a spin-flip process followed by the absorption of a  $\sigma^+$  photon. Consequently, the DR/R signal for a  $\sigma^+$  ( $\sigma^-$ ) probe is proportional to the  $|-1\rangle_{\text{HH}_1}$  ( $|+1\rangle_{\text{HH}_1}$ ) population. The transient signals evidence that the loss of the  $|+1\rangle_{\text{HH}_1}$  excitonic population directly feeds the  $|-1\rangle_{\text{HH}_1}$  pseudospin state via a simultaneous spin flip of electrons and holes. In other words, the time needed to equalize the two signals, corresponding to the two different probe helicities, gives precisely the relaxation time  $\tau_x$  of the exciton spin.<sup>24</sup>

The decays related to the HH<sub>1</sub> exciton exhibit a very similar trend. Here again, when pump and probe are copolarized,



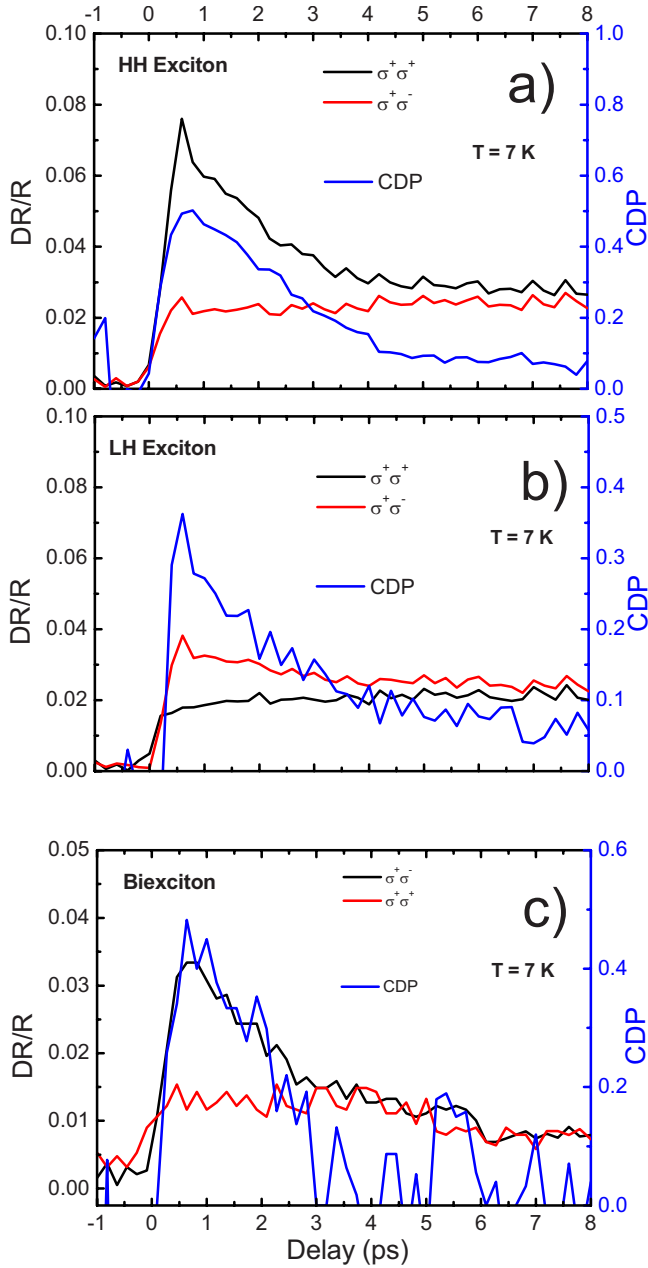


FIG. 4. (Color online) Spectrally integrated DR/R decays for the three transitions: (a)  $\text{HH}_1$ , (b)  $\text{LH}_1$ , and (c) biexciton. The circular degree of polarization (CDP) is also plotted.

the signal reaches its highest value after a risetime in the picosecond range. When the maximum is reached the counterpolarized signal is three times smaller than the copolarized one. Then, the difference between  $\text{DR/R}(\sigma^+\sigma^+)$  and  $\text{DR/R}(\sigma^+\sigma^-)$  tends to zero as fast as the two exciton populations with opposite pseudospin ( $|+1\rangle_{\text{HH}_1}$  and  $|-1\rangle_{\text{HH}_1}$ ) tend to balance. As a consequence of the spin relaxation, the CDP decays exponentially with a time constant close to 2 ps which is quite comparable to the spin lifetime of excitons in GaN epilayers. The optical orientation decay can be due to the spin flip of the exciton as a whole, with a time constant  $\tau_X$ , or to the spin relaxation of the individual carriers, with time constants  $\tau_e$  and  $\tau_h$ . In previous papers devoted to spin

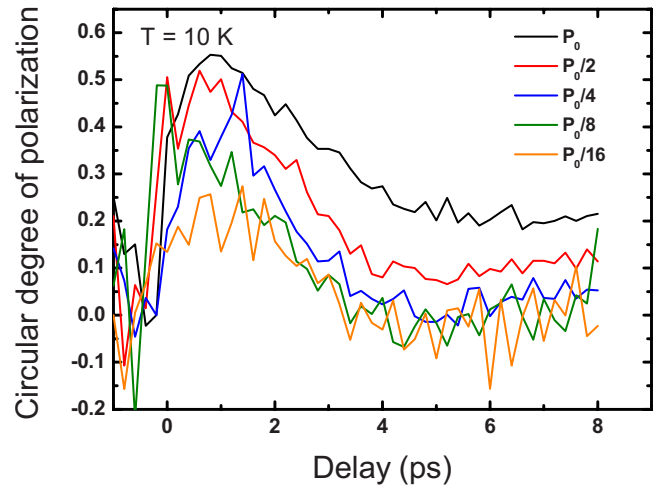


FIG. 5. (Color online) Temporal evolution of the circular degree of polarization, at the  $\text{HH}_1$  exciton energy, for different pump intensities ranging from  $P_0$  to  $P_0/16$ .

dynamics in GaN epilayers,<sup>7,8</sup> we drew the conclusion that the spin relaxation of the individual carriers was more efficient than the exciton spin flip in these systems. In the present case, the similarities between the CDP dynamics at the  $\text{HH}_1$  energy and at the biexciton energy suggest that the spin relaxation mainly occurs because of the spin relaxation of the exciton as a whole.<sup>25</sup> Thus, even if the spin lifetimes in both systems (GaN epilayers and single GaN/AlGaIn QW) are of the same order of magnitude, the physics of spin relaxation is not necessarily identical. Another difference is the initial value of the circular degree of polarization, that can be close to 60%,<sup>26</sup> which is higher than that in bulk material ( $\sim 50\%$  in the case of the best sample in Ref. 8) while being, to our knowledge, the highest value measured in III-nitride compounds. At the  $\text{LH}_1$  exciton energy, the time evolution of the pump-probe signals is comparable to the one of  $\text{HH}_1$  excitons. However, the maximum amplitudes are smaller as already discussed above.

## VI. POWER AND TEMPERATURE DEPENDENCES

In order to gain additional information about the relaxation processes, we have performed experiments for different excitation powers and for different sample temperatures. These complementary studies are limited to the  $\text{HH}_1$ -exciton case, the signal to noise ratio of the other transitions being severely reduced when decreasing the incident power or increasing the sample temperature. Figure 5 displays the time evolution of the CDP for different pump intensities, ranging from  $P_0$  to  $P_0/16$ .  $P_0$  corresponds to an average power equal to  $600 \mu\text{W}$ . No change in the dynamics is observed but the initial value of the CDP is affected. In contrast, the CDP decay times present a strong temperature dependence as shown in Fig. 6. Experiments were carried out from 10 to 120 K. Above the latter temperature, the signal to noise ratio becomes too small to extract reliable quantities. The spin lifetime remains almost constant up to  $\sim 80$  K and then decreases. Above 100 K the relaxation time was shorter than

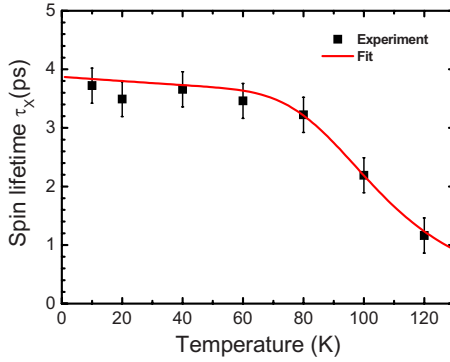


FIG. 6. (Color online) Temporal decay of the circular degree of polarization, at the  $\text{HH}_1$  exciton energy, as a function of temperature.

the experimental time resolution. However, the maximum value of the CDP, reached at zero time delay before any spin flip occurs, remains constant up to 120 K.

## VII. DISCUSSION

We have shown above that the DR/R signals mainly originate from free  $\text{HH}_1$  and  $\text{LH}_1$  excitons, and that the spin relaxation implies a simultaneous flip of both electron and hole spins that connects the two optically active states  $|+1\rangle$  and  $|-1\rangle$  (we will recall in the following how the electron-hole exchange interaction is responsible for the spin flip of an exciton that propagates in a QW). This process was evoked by several groups of authors to interpret spin-dynamics experiments on excitons in GaAs-based QWs.<sup>27</sup> However, as this mechanism appears to be negligible in GaN epilayers,<sup>7,8</sup> we deduce that exchange interaction is considerably larger in the present QWs when compared to the bulk case. From polarization dependent reflectance spectroscopy measurements, Julier *et al.*<sup>28</sup> deduced a value for the spin-exchange energy in wurtzite GaN of  $\gamma \approx 0.6$  meV. Theoretical work has demonstrated that quantum confinement<sup>29–31</sup> can actually enhance exchange interaction provided that the wave vector of the exciton center of mass  $\mathbf{K}$  fulfills the condition  $\mathbf{KL} \gg 1$ , where  $L$  is the well width.<sup>30</sup> Taking into account that the initial, out of equilibrium, population of excitons presents a momentum distribution centered on  $\mathbf{K}=0$ , we assume that elastic exciton-exciton scattering is responsible for the thermalization of excitons to finite  $\mathbf{K}$  states. The thermalization process takes place during the risetime of the nonlinear signal and conserves both energy and total momentum of the two quasiparticles. The energy excess that is equally distributed between excitons is precisely the energy difference between  $\text{HH}_1$  and  $\text{LH}_1$  bands multiplied by the total number of excitons. The final  $\mathbf{K}$  distribution and, therefore, the exchange term in the exciton Hamiltonian that is responsible for the coupling between excitons with opposite pseudospins (see next paragraph) are independent of the exciton density. This is why the experimental dynamics of the DR/R circular degree of polarization is independent of the excitation intensity.<sup>32</sup>

Theoretically, the exchange spin-flip mechanism in QWs was worked out by Maialle *et al.*<sup>33</sup> At finite  $\mathbf{K}$ , the spin-

exchange interaction couples the optically active  $|+1\rangle_{\text{HH}_1}$  and  $|-1\rangle_{\text{HH}_1}$  excitons. The coupling terms in the Hamiltonian can be looked upon as an effective magnetic field about which the exciton pseudospin precesses with a frequency  $\Omega$ . If  $\mathbf{K}$  is kept fixed, the direction of the effective magnetic-field remains constant and the precession leads to spin relaxation when a scattering event occurs that modifies the direction of the  $\mathbf{K}$  vector. Considering the dephasing time  $T_2$ , if the condition  $\Omega T_2 \ll 1$  is fulfilled, the spin relaxation is hindered by motional narrowing as in the D'yakonov-Perel mechanism. Then,  $\tau_X$  can be much larger than  $T_2$  and amounts to:  $\tau_X \sim (\Omega^2 T_2)^{-1}$ . On the contrary when  $\Omega T_2 > 1$ , the spin relaxation rate is proportional to the momentum relaxation rate and  $\tau_X \sim 2T_2$ . We assume the  $T_2$  time in GaN/AlGaIn QWs to be close to the bulk value. Thus, a comparison between the measured value of the spin lifetime  $\tau_X$  in the present QW and the experimental dephasing times in GaN epilayers<sup>34–39</sup> suggests that  $\tau_X$  behaves as  $2T_2$ .<sup>40</sup> Moreover, when increasing the temperature, a dramatic enhancement of the dephasing process is expected through interaction with acoustic and optical phonons.<sup>41</sup> It would lead to an increase in  $\tau_X$  if the relaxation took place in the motional narrowing regime. This is not what is observed in temperature-dependent experiments. We therefore conclude that the spin relaxation of excitons occurs in a regime where  $\Omega T_2 > 1$  as discussed above and that  $\tau_X$  is proportional to  $T_2$ . Understanding spin relaxation implies determining which mechanisms are responsible for the momentum relaxation. This is the purpose of the next paragraphs.

At low temperature, typically between 10 and 50 K, excitons are free to propagate in the QW plane. Even if fluctuations of the confinement potential in the  $x$ - $y$  plane are small, they can scatter the exciton center of mass and consequently, dephase excitons. These fluctuations could be due either to interface roughness or to fluctuations in the barrier alloy concentration. In particular, it has been shown that the former is around 1 nm on a  $5 \times 5 \mu\text{m}^2$  area (rms roughness value) whereas the latter only amounts to 0.2%.<sup>15</sup> Threading dislocations can also play a role in the exciton scattering process because of the Coulomb potential and the strain field that they produce.<sup>42</sup> The experimental manifestation of these scattering processes is the broadening of the main optical transition which is  $\sim 5$  meV for the  $\text{HH}_1$  exciton at 7 K.

At high temperature, a thermally activated process is responsible for the shortening of the dephasing time and therefore of the spin lifetime. In order to extract some quantitative parameters, we fit the temperature evolution of  $\tau_X$  by the expression  $\tau_X = 2T_2 = 2\hbar [\Gamma_0 + a \times T + b \times \exp(-\Delta E/k_B T)]^{-1}$ , where  $\Gamma_0$  is the homogeneous broadening at 0 K,  $a$  stands for the interaction between excitons and acoustic phonons, and  $b \times \exp(-\Delta E/k_B T)$  is the broadening due to a thermally activated process with an activation energy  $\Delta E$ . Longitudinal optical phonons are not taken into account because of the high LO-phonon energy in III-nitrides ( $\sim 92$  meV in bulk GaN). The best agreement between the fit and the experimental data is obtained for  $\Gamma_0 = 0.34$  meV,  $a = 0.32 \mu\text{eV}/\text{K}$ ,  $b = 167.7$  meV, and  $\Delta E = 56.5$  meV. So, when the temperature is increased, the main dephasing mechanism is an escape process of excitons implying energy  $\Delta E = 56.5$  meV. It appears that the situation is very similar to what was obtained

by Brown *et al.*<sup>13</sup> on InGaN/GaN QWs. These authors showed that increasing the temperature enhances the exciton dephasing by interaction through acoustic phonons and by exciton delocalization from potential fluctuations due to alloy disorder. However, even if the intrinsic parameters (exchange interaction, phonon energies) responsible for spin relaxation are close to each other when comparing GaN and InGaN, the two systems are fundamentally different. Indeed, the present GaN quantum well is made of a binary compound and in-plane fluctuations are therefore expected to be much smaller than in InGaN wells leading to small in-plane localization energies. They lie within a few meV as confirmed by the small Stokes shift measured between PL and PLE spectra (3 meV).<sup>18</sup> Consequently, if the thermally activated dephasing process in the present GaN/AlGaIn QW sample was also caused by in-plane delocalization of excitons, it would imply a characteristic energy in the millielectron volt range. This is not the case. On the other hand, as  $\Delta E=56.5$  meV is very close to the energy difference between the fundamental excitonic transitions in the QW ( $HH_1$  and  $LH_1$ ) and that of the AlGaIn barrier (as measured in PL and PLE experiments), we propose the following mechanism to explain the shortening of the spin lifetime at high temperature: when the temperature is increased there is a nonzero probability for QW excitons to escape to the barrier and relax back into the QW. In the meantime, excitons are scattered in the AlGaIn barrier where they relax their momentum and, therefore, their spin. The spin relaxation is then driven by delocalization of exciton from the QW toward the AlGaIn barrier.

### VIII. CONCLUSION

By performing pump-probe experiments, we studied the relaxation dynamics of spin-polarized excitons in a high-quality wurtzite low Al content GaN/AlGaIn quantum well

grown by MOVPE. This enabled us to study free excitons which are responsible for sharp structures in the reflectivity spectrum and strong radiative recombination.

Contrasting with previous results obtained in GaN epilayers, the spin flip of the exciton as a whole seems to be the main spin-relaxation channel in this type of QW. This is thought to originate from the enhancement of the exciton exchange interaction because of quantum confinement, the QCSE being negligible in this QW. The circular degree of polarization of the DR/R signal can reach a value up to 60% for the  $HH_1$  exciton and decays over a time scale of a few picoseconds. This is an indication that, even if excitons are confined in the growth direction, their propagation in the well plane makes them very sensitive to scattering events on potential fluctuations which are responsible for an efficient spin relaxation.

Power-dependent experiments demonstrated that the spin relaxation is left unaffected by the number of photocreated excitons. The spin relaxation process is thermally activated with a characteristic energy  $\Delta E=56.5$  meV showing that excitons are dephased and lose their optical orientation mainly through delocalization into the AlGaIn barrier. However, compared to bulk GaN, the optical orientation is preserved up to  $\sim 100$  K. Therefore, moving toward higher Al content GaN/AlGaIn QWs with a similar optical quality in terms of linewidth could allow both decreasing the spin-relaxation rate and preserving the optical orientation potentially up to room temperature.

### ACKNOWLEDGMENTS

The authors thank A. Boeglin for critical reading of the manuscript. One of the authors (A.G.) thanks the Egyptian ministry of high education and NILES at Cairo University in Egypt for their support in form of a PhD grant at Strasbourg, France. The financial support of the Swiss National Science Foundation through Contract No. 122294 is acknowledged.

\*On leave from NILES, Cairo University, Giza, Egypt.

<sup>†</sup>Corresponding author; mathieu.gallart@ipcms.u-strasbg.fr

<sup>1</sup>I. Vurgaftman, J. R. Meyer, and L. R. Ram-Mohan, *J. Appl. Phys.* **89**, 5815 (2001).

<sup>2</sup>Keeping in mind that for wurtzite semiconductors described in the quasicubic approximation,  $\Delta_{SO}$  is defined as the valence band splitting when the crystal-field splitting  $\Delta_{CR}$  is set to zero, i.e., a situation where the semiconductor recovers a zinc-blende-like band structure.

<sup>3</sup>T. Kuroda, T. Yabushita, T. Kosuge, A. Tackeuchi, K. Taniguchi, T. Chinone, and N. Horio, *Appl. Phys. Lett.* **85**, 3116 (2004).

<sup>4</sup>H. Otake, T. Kuroda, T. Fujita, T. Ushiyama, A. Tackeuchi, T. Chinone, J.-H. Liang, and M. Kajikawa, *Appl. Phys. Lett.* **89**, 182110 (2006).

<sup>5</sup>A. Tackeuchi, H. Otake, Y. Ogawa, T. Ushiyama, T. Fujita, F. Takano, and H. Akinaga, *Appl. Phys. Lett.* **88**, 162114 (2006).

<sup>6</sup>T. Ishiguro, Y. Toda, and S. Adachi, *Appl. Phys. Lett.* **90**, 011904 (2007).

<sup>7</sup>C. Brimont, M. Gallart, O. Crégut, B. Hönerlage, and P. Gilliot, *Phys. Rev. B* **77**, 125201 (2008).

<sup>8</sup>C. Brimont, M. Gallart, A. Gadalla, O. Crégut, B. Hönerlage, and P. Gilliot, *J. Appl. Phys.* **105**, 023502 (2009).

<sup>9</sup>C. Brimont, M. Gallart, O. Crégut, B. Hönerlage, P. Gilliot, D. Lagarde, A. Balocchi, T. Amand, X. Marie, S. Founta, and H. Mariette, *J. Appl. Phys.* **106**, 053514 (2009).

<sup>10</sup>B. Beschoten, E. Johnston-Halperin, D. K. Young, M. Poggio, J. E. Grimaldi, S. Keller, S. P. DenBaars, U. K. Mishra, E. L. Hu, and D. D. Awschalom, *Phys. Rev. B* **63**, 121202(R) (2001).

<sup>11</sup>J. H. Buß, J. Rudolph, F. Natali, F. Semond, and D. Hägele, *Phys. Rev. B* **81**, 155216 (2010).

<sup>12</sup>D. Lagarde, A. Balocchi, H. Carrère, P. Renucci, T. Amand, X. Marie, S. Founta, and H. Mariette, *Phys. Rev. B* **77**, 041304(R) (2008).

<sup>13</sup>J. Brown, J.-P. R. Wells, D. O. Kundys, A. M. Fox, T. Wang, P. J. Parbrook, D. J. Mowbray, and M. S. Skolnick, *J. Appl. Phys.* **104**, 053523 (2008).

- <sup>14</sup>P. Lefebvre, T. Taliercio, S. Kalliakos, A. Morel, X. B. Zhang, M. Gallart, T. Bretagnon, B. Gil, N. Grandjean, B. Damilano, and J. Massies, *Phys. Status Solidi B* **228**, 65 (2001).
- <sup>15</sup>E. Feltin, D. Simeonov, J.-F. Carlin, R. Butté, and N. Grandjean, *Appl. Phys. Lett.* **90**, 021905 (2007).
- <sup>16</sup>Y. Viale, P. Gilliot, O. Cregut, J.-P. Likforman, M. Gallart, B. Hönerlage, K. Kheng, and H. Mariette, *Phys. Rev. B* **69**, 115324 (2004).
- <sup>17</sup>Y. Yamada, Y. Ueki, K. Nakamura, T. Taguchi, Y. Kawaguchi, A. Ishibashi, and T. Yokogawa, *Appl. Phys. Lett.* **84**, 2082 (2004).
- <sup>18</sup>F. S. Cheregi, A. Vinattieri, E. Feltin, D. Simeonov, J.-F. Carlin, R. Butté, N. Grandjean, and M. Gurioli, *Phys. Rev. B* **77**, 125342 (2008).
- <sup>19</sup>“Free excitons” refer here to excitons whose center of mass is free to propagate in the QW plane.
- <sup>20</sup>H. R. Soleimani, S. Cronenberger, M. Gallart, P. Gilliot, J. Cibert, O. Crégut, B. Hönerlage, and J.-P. Likforman, *Appl. Phys. Lett.* **87**, 192104 (2005).
- <sup>21</sup>T. Ostatnický, O. Crégut, M. Gallart, P. Gilliot, B. Hönerlage, and J.-P. Likforman, *Phys. Rev. B* **75**, 165311 (2007).
- <sup>22</sup>F. Stokker-Cheregi, A. Vinattieri, E. Feltin, D. Simeonov, J.-F. Carlin, R. Butté, N. Grandjean, F. Sacconi, M. Povolotskyi, A. Di Carlo, and M. Gurioli, *Phys. Rev. B* **79**, 245316 (2009).
- <sup>23</sup>Note that both the exciton energies and the biexciton binding energy that can be extracted from the data in Fig. 3 are different from those determined from luminescence spectroscopy (Fig. 1). It is due to the fact that the PL measurements and the nonlinear experiment were not performed on the same region of the sample. As exposed in the first paragraph, because of the thickness gradient of the QW, the confinement energy varies across the sample, leading to different energies of the exciton resonances. A stronger confinement also implies a significantly larger binding energy for the biexciton ( $\sim 10$  meV).
- <sup>24</sup>H. R. Soleimani, S. Cronenberger, O. Crégut, J.-P. Likforman, M. Gallart, T. Ostatnický, P. Gilliot, and B. Hönerlage, *Appl. Phys. Lett.* **85**, 5263 (2004).
- <sup>25</sup>In such a circumstance, and if we assume the spin relaxation of the individual carriers to be negligible, the time evolution of the circular degree of polarization takes an analytical form, namely, that of a monoexponential decay characterized by the time constant  $\tau_x/2$ .
- <sup>26</sup>In the figures that are displayed in the present paper, the CDP reaches a maximum value of 55%. However, we have checked that, depending on the experimental conditions, the CDP can reach a value larger than 60%.
- <sup>27</sup>A. Tackeuchi, S. Muto, T. Inata, and T. Fujii, *Appl. Phys. Lett.* **56**, 2213 (1990); Ph. Roussignol, P. Rolland, R. Ferreira, C. Delalande, G. Bastard, A. Vinattieri, L. Carraresi, M. Colocci, and B. Etienne, *Surf. Sci.* **267**, 360 (1992); T. C. Damen, K. Leo, J. Shah, and J. E. Cunningham, *Appl. Phys. Lett.* **58**, 1902 (1991); A. Vinattieri, J. Shah, T. C. Damen, D. S. Kim, L. N. Pfeiffer, M. Z. Maialle, and L. J. Sham, *Phys. Rev. B* **50**, 10868 (1994).
- <sup>28</sup>M. Julier, J. Campo, B. Gil, J. P. Lascaray, and S. Nakamura, *Phys. Rev. B* **57**, R6791 (1998).
- <sup>29</sup>Y. Chen, B. Gil, P. Lefebvre, and H. Mathieu, *Phys. Rev. B* **37**, 6429 (1988).
- <sup>30</sup>L. C. Andreani and F. Bassani, *Phys. Rev. B* **41**, 7536 (1990).
- <sup>31</sup>H. Fu, L.-W. Wang, and A. Zunger, *Phys. Rev. B* **59**, 5568 (1999).
- <sup>32</sup>We assume that the number of photocreated excitons is linear with the pump intensity.
- <sup>33</sup>M. Z. Maialle, E. A. de Andrada e Silva, and L. J. Sham, *Phys. Rev. B* **47**, 15776 (1993).
- <sup>34</sup>A. J. Fischer, W. Shan, G. H. Park, J. J. Song, D. S. Kim, D. S. Yee, R. Horning, and B. Goldenberg, *Phys. Rev. B* **56**, 1077 (1997).
- <sup>35</sup>S. Pau, J. Kuhl, F. Scholz, V. Haerle, M. A. Khan, and C. J. Sun, *Phys. Rev. B* **56**, R12718 (1997).
- <sup>36</sup>R. Zimmermann, A. Euteneuer, J. Möbius, D. Weber, M. R. Hofmann, W. W. Rühle, E. O. Göbel, B. K. Meyer, H. Amano, and I. Akasaki, *Phys. Rev. B* **56**, R12722 (1997).
- <sup>37</sup>S. Pau, J. Kuhl, F. Scholz, V. Haerle, M. A. Khan, and C. J. Sun, *Appl. Phys. Lett.* **72**, 557 (1998).
- <sup>38</sup>T. Aoki, G. Mohs, M. Kuwata-Gonokami, and A. A. Yamaguchi, *Phys. Rev. Lett.* **82**, 3108 (1999).
- <sup>39</sup>H. Haag, B. Hönerlage, O. Briot, and R. L. Aulombard, *Phys. Rev. B* **60**, 11624 (1999); H. Haag, P. Gilliot, R. Lévy, B. Hönerlage, O. Briot, S. Ruffenach-Clur, and R. L. Aulombard, *Appl. Phys. Lett.* **74**, 1436 (1999).
- <sup>40</sup>To the best of our knowledge, no data concerning the dephasing time of excitons in GaN/AlGaN QWs are available. Nevertheless, in GaAs, it was shown that exciton dephasing times in bulk material as well as in QWs are in the picosecond range for a low-excitation density at liquid-helium temperature (Ref. 41 and references therein).
- <sup>41</sup>J. Shah, *Ultrafast Spectroscopy of Semiconductors and Semiconductor Nanostructures*, 2nd ed. (Springer-Verlag, Berlin, 1999).
- <sup>42</sup>D. Jena, *Phys. Rev. B* **70**, 245203 (2004).